The structure of amorphous cellulose as revealed by wide-angle X-ray scattering

Hans-Peter Fink, Burkart Philipp and Dieter Paul
Institute of Polymer Chemistry 'Erich Correns' of Academy of Sciences of GDR, 1530 Teltow-Seehof, German Democratic Republic

and Ritva Serimaa and Timo Paakkari
Department of Physics, University of Helsinki, SF-00170 Helsinki, Finland
(Received 23 June 1986; revised 10 November 1986; accepted 25 November 1986)

The structure of amorphized cellulose samples prepared by ball milling of cellulose I and II and by saponification of cellulose triacetate is investigated by means of radial distribution functions (RDFs). Experimental wide-angle X-ray scattering results are compared with model calculations assuming atomic positions arising from different crystal structure investigations. At small atomic distances ($r < 0.5$ nm) experimentally obtained RDFs and RDFs from models with bent and with twisted backbone conformations are in rather good agreement. Minor peak shifting in this range can be explained by a changing single-chain conformation from cellulose I to cellulose II. For atomic distances $r > 0.5$ nm larger differences exist between experimental and model RDFs, indicating increased distances as compared with the crystalline state.

(Keywords: amorphous cellulose; structure; wide-angle X-ray scattering; radial distribution function)

INTRODUCTION

Conformational order and supermolecular structure of cellulose is a key for understanding the chemical reactions of this natural polymer[1]. The supermolecular structure of cellulose can be considered as a two-phase system with crystalline and non-crystalline arranged chain segments[2,3]. During recent years much experimental and theoretical work has been performed to elucidate the structural features of the ordered, crystalline phases of cellulose. On the other hand, little attention has been paid to the amorphous phase of this polymer. Taking into account the progress in X-ray characterization of amorphous materials in general[4] and especially also of polymers[5-8], the earlier work of Ellefsen *et al.*[9,10] on cellulose amorphized by milling should be continued and sophisticated.

The purpose of this work is to study the structure of amorphous cellulose by means of radial distribution functions (RDFs) derived from wide-angle X-ray scattering (WAXS) patterns. Cellulose samples of crystalline cellulose I and II were amorphized by appropriate ball milling. Additionally, a cellulose sample prepared by saponification of cellulose triacetate was included in our investigations. The chain conformational order and the supermolecular structure of the amorphized cellulose samples were studied by comparing the experimental results and the results of model calculations.

EXPERIMENTAL

Preparation of samples

The starting material of cellulose I was a linters cellulose powder of $DP \approx 180$ obtained by acid hydrolysis and subsequent mechanical disintegration (Filtrak FNA, from VEB Filtrak Niederschlag, DDR). To obtain a sample with cellulose II lattice this FNA powder was treated with 18 wt% of aqueous NaOH at 20°C for 2 h, neutralized, washed and air dried. The order of both samples was decreased by milling them for 250 h in a vibrational stainless-steel ball mill. The decrease of order was followed by X-ray flat-film photographs. It was found that after a milling time of 200 h crystalline order was completely destroyed (*Figure 1*). Increasing disorder due to milling is accompanied by a pronounced decrease in *DP*. For comparison, an amorphous cellulose sample was prepared by saponification of cellulose triacetate ($DS = 2.9$, $M = 50\,000$) with KOH in ethanol to a residual *DS* of 0.001, washing with ethanol and acetone and subsequent drying at 25°C *in vacuo*. In all the steps of preparation, the presence of water was carefully avoided. Our three samples A (from cellulose I), B (from cellulose II) and C (from cellulose triacetate) were kept in a dry box to avoid recrystallization due to air humidity.

WAXS experiments

Measurements were made stepwise using a horizontal diffractometer in symmetric transmission mode according to ref. 11. Both Cu K_α and Mo K_α radiation of wavelength of 0.15418 nm and 0.07107 nm, respectively, monochromatized by means of a flat LiF crystal, were used for the measurements. The diffracted radiation was recorded by a xenon/methane filled proportional counter. A pulse-height analyser was used to eliminate the $\lambda/2$ component in the scattered radiation. The angular range of the measurements was $2° \leqslant \theta \leqslant 52°$ with a step width of 0.1° and $1° \leqslant \theta \leqslant 52°$ with a step width of 0.3° in θ (half of the scattering angle) for Cu K_α and Mo K_α radiation, respectively. For further evaluation the average of two successive runs in fixed time mode has been used. The

0032-3861/87/081265-06$03.00

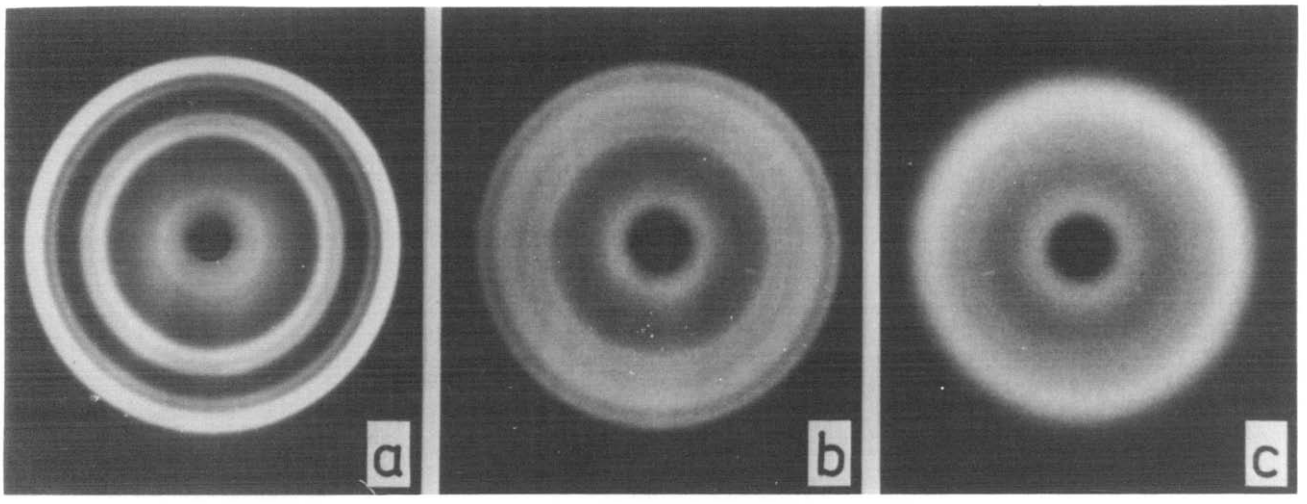

Figure 1 Flat-film X-ray patterns of milled cellulose: (a) starting material (FNA powder); (b) FNA powder milled for 50 h; (c) FNA powder milled for 250 h

relative statistical error was less than 1.4% for Cu K_α radiation and less than 2% for Mo K_α radiation. Stability of the equipment, including the X-ray source, was checked by measuring the scattered intensity of a polyethylene calibration sample at a fixed scattering angle.

Cellulose samples were placed between 15 μm polyester foils as a flat cake of 2 mm thickness. Measurements of the attenuation factor of the sample were performed by the aid of the calibration sample with and without the cellulose sample in the incident beam. Parasitic scattering, including that from the foils, was measured using a no-sample arrangement.

THEORY AND ANALYSIS OF DATA

Theoretical background for obtaining RDF from WAXS

Only the formulae necessary to understand the treatment of the data and the discussion of the results will be given here, according to refs. 12 and 13. The RDF, $D(r)$, of an isotropic sample is defined as a weighted superposition of electron densities $\rho_m(r)$ for each kind of atom in the structural unit at distance r from an average atom of type m:

$$D(r)=4\pi r^2\sum_m K_m\rho_m(r) \tag{1}$$

The sum in (1) has to be taken over the structural unit and the weighting factors, K_m, are defined by

$$f_m=K_m f_e \tag{2}$$

where f_m is the scattering factor of the atom of kind m and f_e is an average scattering factor per electron in the structural unit. The RDF can now be calculated from the equation

$$D(r)=4\pi r^2\rho_0\sum_m K_m+\frac{2r}{\pi}\int_0^\infty si(s)\sin(rs)\,ds \tag{3}$$

where ρ_0 is the average electron density and $s=(4\pi/\lambda)\sin\theta$ is the value of the scattering vector. The reduced intensity $i(s)$ is connected to the experimentally determined coherent intensity $I(s)$ by

$$i(s)=\left(I(s)/N-\sum_m f_m^2(s)\right)f_e^{-2} \tag{4}$$

The summation in (4) is again taken over the structural unit and N is the number of these structural units in the sample. The reduced radial distribution function $D^*(r)$ is defined by

$$D^*(r)=D(r)-4\pi r^2\rho_0\sum_m K_m \tag{5}$$

Data treatment

First, the experimental data were corrected for parasitic scattering, including that from the polyester foils, for absorption and for scattering volume and polarization. The large-angle part of the data was then smoothed using a procedure based on running averages. In the second step the values of the measured and corrected intensity, $I^{corr}(s)$, were normalized to the intensity of an appropriate structural unit [four anhydroglucose units (AGUs), i.e. 20 oxygen, 24 carbon and 40 hydrogen atoms]. In the third step of the data treatment the RDF is calculated according to equation (3).

The intensity, $I^{calc}(s)$, independently scattered by the atoms of the chosen structural unit, was calculated using interpolated values from refs. 14 and 15:

$$I^{calc}(s)=\sum_m f_m^2(s)+A(s)B\sum_m I_m^{inc}(s) \tag{6}$$

The sum of Compton intensities $I_m^{inc}(s)$ was corrected by an absorption factor, $A(s)$, to take into account extra absorption due to the wavelength shift[8,16]. The factor B corrects for multiple Compton scattering. By Monte Carlo calculations[17] for a cellulose sample in the geometry used and for Mo K_α radiation, the value of $B=1.06$ was obtained as a first approximation.

To normalize the experimental data, I^{corr}, both the

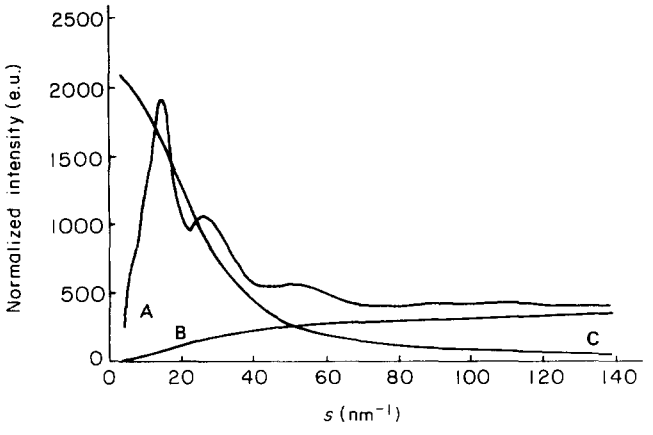

Figure 2 Normalized experimental and independent scattering curves for milled cellulose I (sample A): curve A, experimental intensity CI^{corr}; B, incoherent scattering; C, independent coherent scattering

integral method[18,19]

$$C=\frac{\int_{s_1}^{s_2} I^{calc}(s)s^2\,ds}{\int_{s_1}^{s_2} I^{corr}(s)s^2\,ds} \qquad (7)$$

and the large-angle method

$$C=(1/N)\sum_{i=1}^{N} I^{calc}(s_i)/I^{corr}(s_i) \qquad \text{for } s_i>s_0 \qquad (8)$$

were used. For $s_2>120\,nm^{-1}$ the resulting normalization constant, C, from (7) was independent of the upper limit of integration. This result as well as the good agreement between the values of C obtained from (7) and (8) (difference smaller than 2%) indicated a high reliability of normalization in the case of measurements made by Mo K_α radiation. In the case of Cu K_α measurements the reduced range of s resulted in differences smaller than 6% between both methods of normalization as well as some dependence on the value of s_2. *Figure 2* gives an impression of the relations between the normalized intensity $CI^{corr}(s)$ and the two contributions of the independently scattered intensities in equation (6). After normalization the reduced intensities were calaculated from

$$i(s)=[CI^{corr}(s)-I^{calc}(s)]\sum_m f_m^2(0)\Big/\sum_m f_m^2(s) \qquad (9)$$

where the last factor corresponds to f_e^{-2} in (4). The RDF and the reduced RDF were then calculated using (3) and (5) and a fast Fourier transform procedure. Assuming only independent scattering after the experimental limit $s_2=139\,nm^{-1}$, the step width of $\Delta s=0.5\,nm^{-1}$ corresponds to $r=0.01$ nm with 1250 steps in real space. The influence of any termination effects on the position of the peaks was carefully checked to be negligible. No damping was also applied except in the close vicinity of the termination point to avoid the influence of any statistical errors.

Model calculations

To calculate the reduced intensities due to some molecular models of cellulose the following interference term of the Debye formula was used:

$$i(s)=\sum_{\substack{n,m\\ n\neq m}} f_m f_n \sin(sr_{mn})/sr_{mn}-i_{SAXS}(s) \qquad (10)$$

Small-angle scattering $i_{SAXS}(s)$ due to the finite size of the molecular models employed was calculated assuming a cylindrical shape of the structural unit[20]. In every case, only carbon and oxygen atoms have been considered, neglecting the minor contribution of hydrogen atoms. Model intensities have been treated in the same way as measured reduced intensities to obtain the corresponding RDFs and the reduced RDFs.

RESULTS

Results are presented and discussed in reciprocal space as well as in real space taking advantage of both modes (cf. refs. 5 and 21). For discussion in reciprocal space the function $si(s)$ is preferred because it is directly related to the reduced RDF by the Fourier transform.

The $si(s)$ functions obtained from Cu K_α radiation measurements for the milled samples A and B are shown in *Figure 3*. Corresponding reduced RDFs $D^*(r)$ are plotted in *Figure 4*. Measurements with Mo K_α radiation

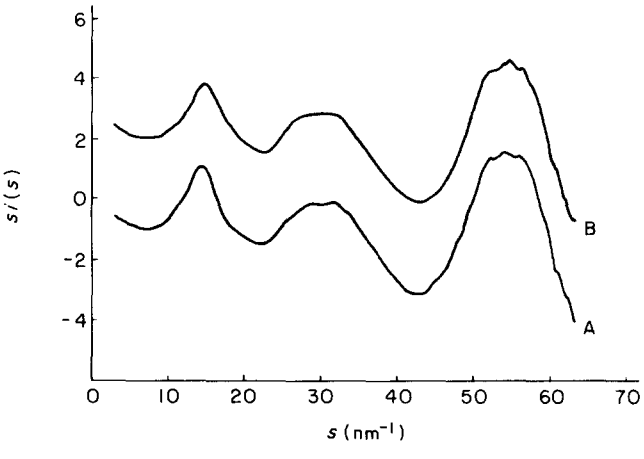

Figure 3 s-Weighted reduced intensity functions $si(s)$ of samples A and B from Cu radiation experiments (curve B is shifted arbitrarily on the ordinate axis)

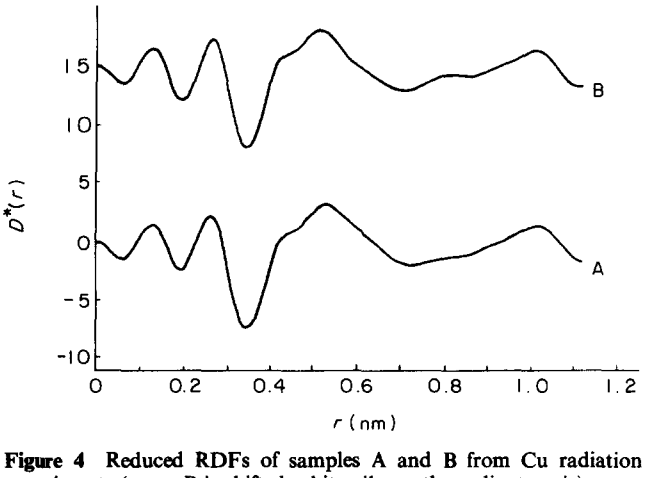

Figure 4 Reduced RDFs of samples A and B from Cu radiation experiments (curve B is shifted arbitrarily on the ordinate axis)

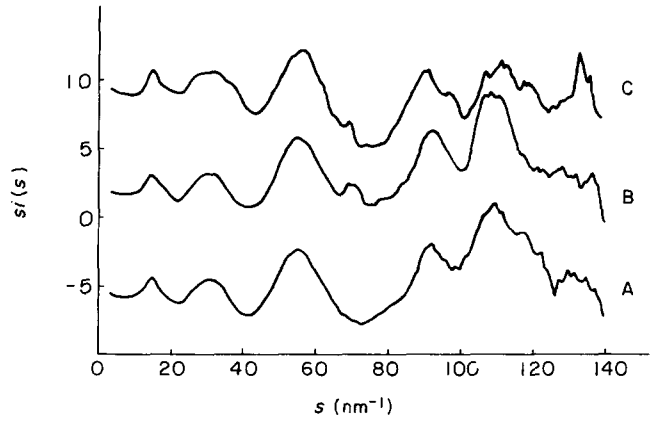

Figure 5 s-Weighted reduced intensity functions $si(s)$ of samples A, B and C from Mo radiation experiments (curves are shifted arbitrarily on the ordinate axis)

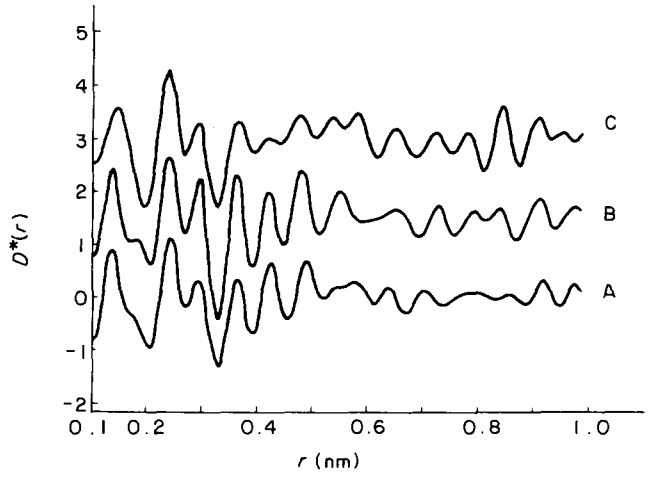

Figure 6 Reduced RDFs of samples A, B and C from Mo radiation experiments (curves B and C are shifted arbitrarily on the ordinate axis)

provide an extended range of s values as demonstrated in the plot of $si(s)$ *versus* s in *Figure 5*. *Figure 6* shows the corresponding functions $D^*(r)$ for the samples A, B and C. Interatomic distances as obtained from peak positions of the reduced RDFs are summarized in *Table 1*.

DISCUSSION

In the range $s \lesssim 60\,\text{nm}^{-1}$ scattering curves from both Cu radiation and Mo radiation experiments are available for the milled samples A and B. In this range there are no significant differences between the $si(s)$ curves of the samples (compare *Figures 3* and *5*). Reduced RDFs arising from Cu K_α radiation measurements (*Figure 4*) are nearly identical for milled samples of cellulose I and II, showing broad peaks in the range 0.1–0.2 nm, 0.2–0.3 nm, at about 0.5 nm and around 1.0 nm. Up to this point the present results agree well with the results of Ellefsen *et al.*[9,10], which means that no differences between milled cellulose I and II can be detected using Cu K_α radiation. From their results Ellefsen *et al.*[10] concluded that the RDF of amorphous cellulose essentially depends on the spatial arrangement of successive AGUs in the chain molecule and that there is an irregular packing of rods of a diameter of ≈ 0.5 nm.

Taking into account the relatively small resolution $\delta r = 2\pi/s_{max} \approx 0.1$ nm of the Cu K_α experiments, no further details of short-range order should be expected. But, depending on the chosen step width Δs, those experiments with Cu K_α radiation may provide reasonable results to the middle range order (up to 2 nm) of cellulose, a topic we are not concerned with in this paper.

Changing to Mo K_α radiation, small but meaningful differences between the $si(s)$ curves of the samples can be seen at higher values of the scattering vector (*Figure 5*). Especially, an additional peak was detected in the curves of samples B and C at $s = 70\,\text{nm}^{-1}$. As expected, the resolution of the RDFs is increased (*Figure 6*) by using Mo Kα radiation.

To check the meaningfulness of the peaks in the experimental RDFs (*Figure 6*) the distances indicated by the peak positions (*Table 1*) were compared with calculated interatomic distances (*Table 2*) of a single-chain model (*Figure 7*) used for crystal structure analysis[22]. The interatomic distances (without hydrogen atoms) calculated for one cellobiose unit of the assumed model conformation fall into six groups within the total range $0.1\,\text{nm} < r < 0.5\,\text{nm}$ (*Table 2*). The average positions of these groups generally coincide with the observed peaks in this range of reduced RDFs (compare *Tables 1* and *2*), indicating that there is no 'spurious' peak. Comparing the reduced RDFs of the three samples, no differences in peak positions are detectable for $r < 0.36$ nm. Small differences between the samples may be recognized for $0.4\,\text{nm} < r < 0.5\,\text{nm}$. The peaks observed in RDF of sample A at about 0.43 and 0.49 nm are shifted to smaller values for samples B and C. Still larger differences between the samples do exist in the range $r > 0.5$ nm. It seems reasonable to assume that intramolecular (intrasegmental) distances dominate for $r < 0.5$ nm. For $r > 0.5$ nm both intramolecular and intermolecular (intersegmental) distances are to be taken into account.

To discuss the features of measured intensities and resulting RDFs, a comparison with model intensities and model RDFs should be useful. Model calculations were performed for different single-chain conformations (variation of intramolecular distances) and different chain packing (variation of intermolecular distances). Calculations of $si(s)$ and $D^*(r)$ were performed taking into account atomic positions according to the following

Table 1 Interatomic distances (nm) in the measured reduced RDFs

Peak	Sample A	Sample B	Sample C
1	0.14	0.14	0.14
2	0.24	0.24	0.24
3	0.29	0.29	0.29
4	0.36	0.36	0.36
5	0.43	0.42	0.42
6	0.49	0.48	0.48
7			0.53
8	0.58	0.55	0.57
9	0.64	0.65	0.65
10	0.70	0.73	0.72
11	0.79	0.79	0.78
12	0.86	0.83	0.84
13	0.91	0.91	0.91
14			0.95
15	1.03	1.00	1.03
16	1.08	1.07	1.11

Table 2 The shortest interatomic distances (nm) of atoms in cellulose I

Peak 1		Peak 2		Peak 3	
C1–C2	0.152	C1–C3	0.251	C1–C4	0.289
C1–O1	0.139	C1–C5	0.238	C2–C5	0.286
C1–O5	0.143	C1–O2	0.240	C3–O5	0.287
C2–C3	0.152	C1–C4	0.237	O1–O2	0.281
C2–O2	0.143	C2–C4	0.249	O2–O3	0.289
C3–C4	0.152	C2–O1	0.237	O1–C6′	0.294
C3–O3	0.143	C2–O3	0.241	O1–O3′	0.290
C4–C5	0.152	C2–O5	0.241	O1–O6′	0.290
C5–C6	0.152	C3–C5	0.249	O2–O3	0.289
C5–O5	0.144	C3–O2	0.243	O2–O6′	0.288
C6–O6	0.144	C4–C6	0.253	O5–O3′	0.274
O1–C4′	0.143	C4–O3	0.241		
		C4–O5	0.243		
		C5–O6	0.244		
		C6–O5′	0.237		
		O1–O5′	0.227		
		O1–C3′	0.242		
		O1–C5′	0.240		
Peak 4		**Peak 5**		**Peak 6**	
C1–C6	0.368	C2–C6	0.425	C1–O6	0.477
C1–O3	0.375	C4–O1	0.413	C6–O1	0.464
C3–C6	0.386	C5–O2	0.415	C6–O3	0.493
C3–O1	0.371	O3–O5	0.413	O1–O3	0.477
C4–O2	0.376	C2–C6′	0.429	C1–C2′	0.457
C5–O1	0.375	C6–O3′	0.405	C1–O5′	0.473
C5–O3	0.375	O1–C1′	0.415	C2–C3′	0.463
O2–O5	0.365	O2–C5′	0.421	C2–O3′	0.461
O5–O6	0.362	O3–O5	0.413	C3–C4′	0.482
C1–C5′	0.358			C5–C3′	0.461
C1–C6′	0.386			O1–O2′	0.483
C1–O6′	0.376			O5–C2′	0.478
C2–C4′	0.359				
C2–O6′	0.371				
C5–O3′	0.374				
O1–C2′	0.375				
O1–O5′	0.367				
O2′–C4′	0.377				
O2–C6′	0.357				
C5–O3′	0.374				

models (*Figure 7*):

(a) Gardner and Blackwell[22], cellulose I, bent conformation;

(b) Kolpak and Blackwell[23], cellulose II, centre chain, bent conformation;

(c) Watanabe and Hayashi[24], cellulose II, bent and twisted conformation.

The simplest conceivable model for amorphous cellulose is a single-chain model with straight cellulose chains isotropically distributed in the sample. For this case and model (a) the influence of increasing chain length on the $si(s)$ curve is demonstrated in *Figure 8*. With increasing chain length a size effect resulting in peak splitting can be observed. Especially, an extra peak in the range $60 < s < 70\,nm^{-1}$ results from this model operation. From this consideration and the generally good agreement between the model curves in *Figure 8* and the experimental curves in *Figure 5*, the conclusion may be drawn that the length of straight chain segments in sample A is probably smaller than in samples B and C.

Some influence on peak positions in model RDFs should be expected using different backbone conformations (models (a) and (b) *versus* model (c)) and simulating packing effects. RDF calculations were performed using models (a), (b) and (c) assuming either (i) isolated straight chains of 24 AGUs, or (ii) four chains, every one built up of six AGUs each, arranged as two corner chains and two centre chains just as in the appropriate unit cell of crystalline cellulose. Resulting interatomic distances of model RDFs are shown in *Table 3*. In the range of distances $r < 0.5$ nm only small differences exist between the models, and the same holds true for a comparison between model calculations and experimental results (compare *Table 1*). Larger differences are found for $r > 0.5$ nm between the models as well as between model calculations and experimental results. From this it may be concluded that the distances between the chains are increased in comparison with those in a crystalline state. A comparison of RDFs of samples B and C and single-chain models (b) and (c) is shown in *Figure 9*. Here, for peak positions in the range $0.4\,nm < r < 0.5$ nm the experimental results agree better with model (c). This means that the observed shifting of these peaks connected with the changes from sample A to samples B and C may be explained by a changing backbone conformation from bent to bent and twisted type.

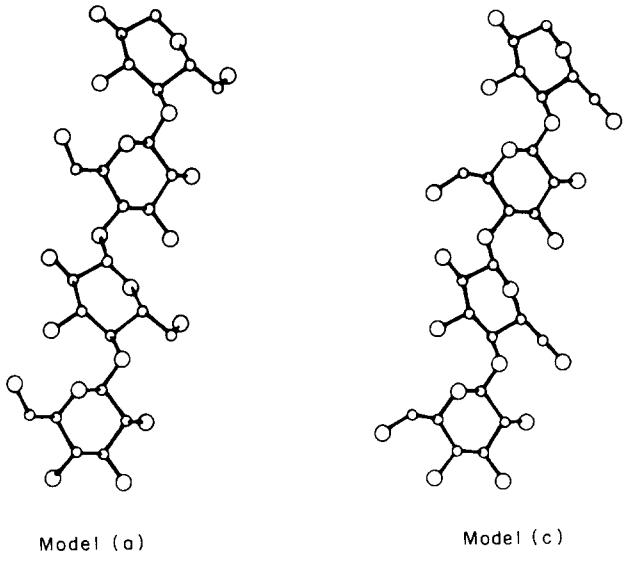

Figure 7 Computer-generated pictures of cellulose molecular models with bent backbone conformation[22] (model (a)) and bent and twisted backbone conformation[24] (model (c))

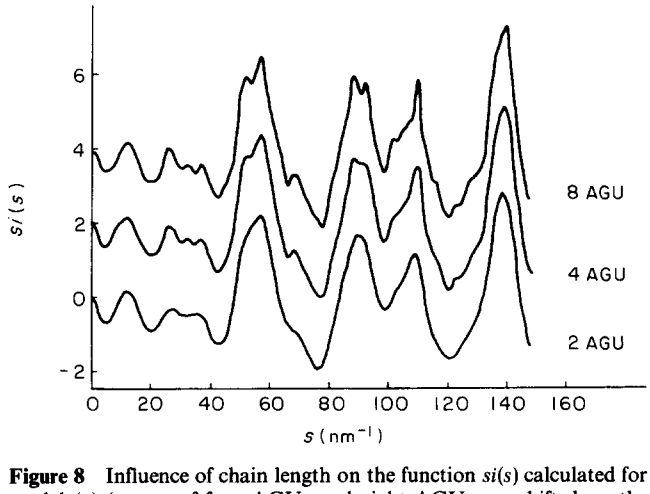

Figure 8 Influence of chain length on the function $si(s)$ calculated for model (a) (curves of four AGUs and eight AGUs are shifted on the ordinate axis)

Table 3 Interatomic distances (nm) in model reduced RDFs

Model (a)		Model (b)		Model (c)	
Single chain	Four chains	Single chain	Four chains	Single chain	Four chains
0.15	0.15	0.15	0.15	0.15	0.15
0.24	0.24	0.24	0.24	0.24	0.24
0.30	0.29	0.30	0.30	0.30	0.30
0.37	0.37	0.37	0.37	0.37	0.37
0.43	0.43	0.43	0.43	0.42	0.4
0.48	0.49	0.49	0.49	0.48	0.48
0.54	0.56	0.57	0.56	0.57	0.57
0.58					
0.66	0.64	0.65	0.65	0.65	0.65
	0.70				
0.80	0.77	0.77		0.76	
	0.82	0.81	0.76	0.81	0.8
0.87	0.89	0.89	0.81	0.88	0.89
0.93	0.94	0.93	0.89	0.93	
0.99					
1.03	1.03	1.03	1.03	1.03	1.03
1.10	1.10			1.10	
1.15	1.15	1.15	1.15	1.15	1.14

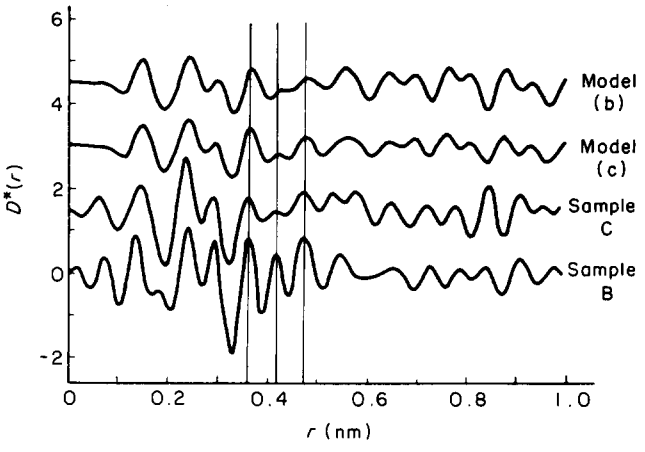

Figure 9 Comparison of reduced RDFs derived from samples B and C and models (b) and (c) (upper three curves are shifted on the ordinate axis)

REFERENCES

1 Philipp, B. *Österr. Chem. Z.* 1985, **5**, 96
2 Fink, H.-P., Fanter, D. and Philipp, B. *Acta Polym.* 1985, **36**, 1
3 Fink, H.-P. and Philipp, B. *J. Appl. Polym. Sci.* 1985, **30**, 3779
4 Hargittai, I. and Orville-Thomas, W. J. (Eds.), 'Diffraction Studies on Non-Crystalline Substances', Elsevier Scientific, Amsterdam, 1981
5 Lovell, R., Mitchell, G. R. and Windle, A. H. *Faraday Disc.* 1979, **68**, 46
6 Mitchell, G. R., Lovell, R. and Windle, A. H. *Polymer* 1980, **21**, 989
7 Wignall, G. D. and Longman, G. W. *J. Mater. Sci.* 1973, **8**, 1439
8 Longman, G. W., Sheldon, R. P. and Wignall, G. D. *J. Mater. Sci.* 1976, **11**, 1339
9 Ellefsen, Ø., Lund, E. W., Tønnesen, B. A. and Øien, K. *Norsk Skogindustri* 1957, **11**, 284
10 Ellefsen, Ø., Kringstadt, K. and Tønnesen, B. A. *Norsk Skogindustri* 1964, **18**, 419
11 Herms, G. and Hajdu, F. *J. Appl. Crystallogr.* 1984, **17**, 140
12 Warren, B. E. 'X-ray Diffraction', Addison-Wesley, Reading, Mass., 1969
13 Klug, H. P. and Alexander, L. E. 'X-ray Diffraction Procedures for Polycrystalline and Amorphous Materials', Wiley, New York, 1974
14 Hubbell, J. H., Veigele, Wm. J., Briggs, E. A., Brown, R. T., Cromer, T. A. and Howerton, R. J. *J. Phys. Chem. Ref. Data* 1975, **4**, No. 3
15 Alexandropoulos, N. G. and Cooper, M. J., Contribution to the new edition of 'International Tables for Crystallography'
16 Hajdu, F. and Palinkas, G. *J. Appl. Crystallogr.* 1972, **5**, 395
17 Halonen, V., Williams, B. G. and Paakkari, T. *Phys. Fenn.* 1975, **10**, 107
18 Krogh-Moe, J. *Acta Crystallogr.* 1956, **9**, 951
19 Norman, N. *Acta Crystallogr.* 1957, **10**, 370
20 Guinier, A. and Fournet, G. 'Small-Angle Scattering of X-Rays', Wiley, New York, 1955
21 Ruland, W. *Pure Appl. Chem.* 1969, **18**, 489
22 Gardner, K. H. and Blackwell, J. *Biopolymers* 1974, **13**, 1975
23 Kolpak, F. J. and Blackwell, J. *Macromolecules* 1976, **9**, 273
24 Watanabe, S. and Hayashi, J. *Kogyo Kagaku Zasshi* 1970, **73**, 1890